Cellulose (2015) 22:3117–3126
DOI 10.1007/s10570-015-0691-2

ORIGINAL PAPER

Properties of hydroxypropyl guar/TEMPO-oxidized cellulose nanofibrils composite films

Lei Dai · Bin Wang · Zhu Long · Le Chen · Dan Zhang · Shuai Guo

Received: 2 March 2015 / Accepted: 22 June 2015 / Published online: 26 June 2015

Abstract Flexible hydroxypropyl guar/TEMPO-oxidized cellulose nanofibrils (HPG/TOCNs) composite films were prepared using a conventional solvent-casting technique. Their properties were investigated with a variety of techniques including tensile test, Fourier-transform infrared spectroscopy, scanning electron microscopy, oxygen permeability test, water vapor permeability test, thermogravimetric analysis and water contact angle measurement. The results indicate that HPG and TOCNs have an excellent miscibility and their blending mass ratio can significantly affect the physical, thermal, oxygen barrier and water vapor barrier properties of the composite films. Compared with pure HPG film, the composite films exhibit higher tensile strength and oxygen barrier properties. The water vapor resistance and thermal stability of the composite films are slightly lower than those of HPG film. However, the excellent flexibility, transparency and gas-barrier properties of the environmentally friendly HPG/TOCNs composite film make it a promising packaging material for food and pharmaceutical industries.

Keywords Cellulose nanofibrils · Hydroxypropyl guar · Composite film · TEMPO · Oxygen barrier · Water vapor permeability

L. Dai · Z. Long (✉) · L. Chen · D. Zhang · S. Guo
Laboratory of Papermaking, School of Textiles & Clothing, Jiangnan University, Wuxi 214122, China
e-mail: longzhu@jiangnan.edu.cn

L. Dai · Z. Long · L. Chen · D. Zhang · S. Guo
Key Laboratory of Eco-textiles, Ministry of Education, Jiangnan University, Wuxi 214122, China

B. Wang
State Key Lab of Pulp and Paper Engineering, South China University of Technology, Guangdong Public Laboratory of Paper Technology and Equipment, Guangzhou 510640, China

Introduction

Cellulose nanofibrils (CNs) have attracted considerable attention in recent years due to their biodegradability, large surface area, high strength and high film-forming capacity (Rodionova et al. 2012a). It is a highly reproducible and environmentally friendly nanomaterial (Fujisawa et al. 2011) and has been used as the nano-fillers (Iwatake et al. 2008), thin coating layers (Aulin and Strom 2013), and films (Song et al. 2014) for many generic and cutting-edge products. Cellulose nanofibrils are usually prepared from native cellulose fibers through 2,2,6,6-tetramethylpiperidine-1-oxyl (TEMPO)-mediated oxidation and successive mild shear mechanical treatment (Saito et al. 2006, 2007). Compared with native cellulose fibers, TEMPO-oxidized cellulose nanofibrils (TOCNs) is deemed as an innovative nano-sized biomaterial due to its crystalline and amorphous domains (Jradi et al. 2012). TOCNs prepared from wood cellulose are 3–4 nm wide nanofibers with high aspect ratios of >50

and can be individually dispersed in water (Fujisawa et al. 2011). Self-standing films made by casting and drying aqueous TOCNs dispersions are very flexible and transparent (Fukuzumi et al. 2009). In addition, the oxygen permeability (OP) of TOCNs film is only 0.049 mL μm m^{-2} day^{-1} kPa^{-1} (Fujisawa et al. 2011), which is lower than that of poly(vinyl alcohol) (PVA) (Kato et al. 2005).

TOCNs can be blended with water-soluble polymers such as PVA (Zhou et al. 2012), poly(ethylene oxide) (Fukuya et al. 2014) and poly(acrylamide) (Kurihara and Isogai 2014) to prepare highly flexible and strong composites since TOCNs have high dispersibility in water (Sirvio et al. 2014; Wu et al. 2012; Kurihara and Isogai 2014). The "nano-effects", referring to the phenomenon that the composites properties improve significantly with the incorporation of nano-element, occurred during the blending can improve the performance of the produced TOCNs composite films. In addition, layer-by-layer coated film of chitin nanofibrils/TOCNs (Qi et al. 2012) and oxidized starch/TOCNs composite film (Kurihara and Isogai 2014) prepared with water as a dispersion medium, show excellent mechanical properties and significantly different properties from those of the composites without TOCNs. Therefore, the incorporation of TOCNs into the modified composite films can expand their applications.

Hydroxypropyl guar (HPG) is a water-soluble nonionic polysaccharide consisting of a linear backbone of β-(1-4) D-mannose units with α-(1-6) D-galactose units randomly attached as side chains (Nayak and Singh 2001). It has better water solubility and film forming property than guar gum (Lu et al. 2005; Xiao et al. 2003) and plays a large role in the various products of chemically modified guar gum (Cheng et al. 2002). HPG has been widely used in many industries such as oil recovery, food industry, paints and the formulation of cartridge explosives (Wu et al. 2010; Xiao et al. 2003). The large amount of –OH groups in HPG can interact with sodium carboxylate groups and hydroxyl groups on the surfaces of TOCNs. These attractive interactions may result in a well-blended composite material with improved properties.

In the present work, composite films with various blending mass ratios of HPG to TOCNs were prepared through solution casting method. The miscibility, physical properties and thermal properties of the composite films were determined with tensile measurements, Fourier transform infrared spectroscopy (FTIR), scanning electron microscopy (SEM) and thermogravimetric analysis (TGA). The oxygen and water vapor barrier properties were also examined. The effects of the blending ratio between TOCNs and HPG on the properties of the composite films were investigated. The results reported in this article may contribute to finding further applications of these composite films in package materials.

Experimental

Materials

A commercial softwood bleached kraft pulp (SBKP) was pretreated with 5 % (v/v) formic acid solution to improve the efficiency of TEMPO-mediated oxidation (Dai et al. 2014). Hydroxypropyl guar (HPG) with a degree of substitution (DS) of 0.15 was kindly provided by Wuxi JinXin Group Co., Ltd. (Wuxi, China). All other reagents were purchased from Sinopharm Chemical Reagent Co., Ltd. (Shanghai, China) and used as received.

TEMPO-oxidized cellulose nanofibrils (TOCNs) production

The formic acid pretreated pulp (5 g) was suspended in a 500 mL solution containing 0.1 g TEMPO, 1.0 g NaBr, 3.71 g Na_2CO_3 and 1.26 g $NaHCO_3$. Thereafter, NaClO (4.5 mmol/g pulp) was added to the suspension under ambient condition to prepare TEMPO-oxidized cellulose. The oxidation reaction was quenched by adding 10 mL ethanol after 4 h. The carboxylate content of TEMPO-oxidized cellulose was 1.34 mmol g^{-1}. An aqueous 1 wt% TEMPO-oxidized cellulose slurry was homogenized with an IKA T25 digital ULTRA-TURRAX homogenizer at 20,000 rpm for 30 min and subsequently sonicated with an ultrasonic probe (25 mm probe tip diameter, Scientz, China) at 19.5 kHz and 400 W for 20 min. The transparent TOCNs aqueous dispersion was stored at 4 °C before use.

Preparation of HPG/TOCNs composite films

Ten grams HPG powder was completely dissolved in 1000 mL deionized water at room temperature by

stirring at 300 rpm for 8 h. Then, the HPG solution was mixed with TOCNs aqueous dispersion with the dry mass ratios of 100:0, 70:30, 50:50, 30:70 and 0:100. The mixtures were stirred for 3 h and poured into polytetrafluoroethylene petri dishes (150 mm diameter), respectively. The films were oven-dried at 50 °C for 3 days, peeled off and marked as HPG (100:0), CF1 (70:30), CF2 (50:50), CF3 (30:70) and TOCNs (0:100), respectively. All these films were kept at 23 °C and a relative humidity (RH) of 50 ± 1 % for 2 days before characterization.

Thickness/density measurement

Film thickness was determined as an average of ten measurements using a thickness meter (MP0, Fischer, Germany). Density of individual film was calculated by dividing grammage by film thickness.

UV–Vis transmittance

The light transmittance of the films was characterized with a Shimadzu UV-1800 UV–Vis spectrometer, and was measured from 200 to 800 nm.

Mechanical test

The films were cut into 10 mm × 100 mm rectangular strips and their tensile strength and elongation at break were measured at room temperature with a BZ2.5/TNIS Zwick Material Tester (Zwick, Germany). The initial grip separation was set at 50 mm and specimens were loaded at a constant cross-head speed of 50 mm/min. At least 5 specimens of each sample were tested.

Fourier-transform infrared (FTIR) spectroscopy

FTIR spectra of all films were recorded on a Nicolet is 10 spectrometer with an attenuated total reflectance (ATR) accessory (Thermo Fisher Scientific Inc., USA) at a resolution of 4 cm^{-1} in the range of 550–4000 cm^{-1}. An average of 16 scans was reported.

Scanning electron microscopy (SEM)

The cross-sections of the films were affixed to a vertical brass specimen holder for the SEM imaging. Samples were coated with a gold layer and their surface morphologies were examined with a HITACHI SU1510 SEM at 5 kV acceleration voltage.

Contact angle (CA) measurement

The water contact angle of each film was measured with a Drop Shape Analyzer-DSA 100 (KRUSS GmbH, Germany) at ambient condition. A drop of water (4 μL) was deposited on the specimen surface and a series of water droplet images were captured and analyzed.

Oxygen permeability

The oxygen permeability of the films was determined with a Labthink VAC-V1 apparatus (Labthink, China) at 23 °C and 40 ± 1 % RH. The sample size was 38.48 cm^2 and the partial pressure of oxygen was 0.1 MPa.

Water vapor permeability (WVP)

The WVP of the films was determined according to the previous reports (Das et al. 2011; Sharma et al. 2014). Briefly, a composite film with an area of 19.64 cm^2 was sealed on a cup containing 10 g of oven-dried $CaCl_2$ as a desiccant. The cup covered with sample was accurately weighted and put in a desiccator cabinet containing saturated NaCl solution that was used to generate 75 % RH gradient. The cup covered with film was reweighted every 24 h until a constant weight was obtained. The WVP was calculated using the following equation:

$$\mathrm{WVP} = \frac{\Delta m \times \delta}{\Delta t \times A \times \Delta P}$$

where Δm/Δt is the moisture weight of the film gained per time unit, δ is the average film thickness, A is the exposed surface area of the specimen, ΔP is the difference between the water vapor pressures on the two sides of the specimen. All measurements were repeated three times and only the mean value was reported.

Thermogravimetric analysis (TGA)

TGA of films was conducted on a TGA/SDTA 851e Thermoanalyzer (METTLER TOLEDO, Switzerland). The samples were heated from 25 to 600 °C at

a heating rate of 10 °C/min. A nitrogen gas stream was continuously passed into the furnace at 10 mL/min and the gradual weight loss of the sample was recorded.

Results and discussion

Optical and mechanical properties

All films were translucent, smooth, flexible and relatively tough. Figure 1 shows the photographs of HPG, CF1, CF2, CF3 and TOCNs films. Obviously, there exists visual difference between the films with different composition ratios. In addition, light transmittance through the films as a function of wavelength was obtained and is shown in Fig. 2. The transmittance at 600 nm was around 85 % for TOCNs film, while it was about 52 % for the HPG film. The transparency of the composite films was increased with a higher amount of TOCNs. It is well known that the particles with diameters less than one-tenth of the visible-light wavelength do not scatter light (Yang et al. 2012; Yano et al. 2005). Therefore, the high transparency of the TOCNs film can be attributed to the nano-sized fibers of TOCNs (Rodionova et al. 2012c) while the lower transmittance of HPG film is probably due to the remaining cell wall fragments. Otherwise, the introduction of HPG into the composite films increased the particle size, leading to increased light scattering.

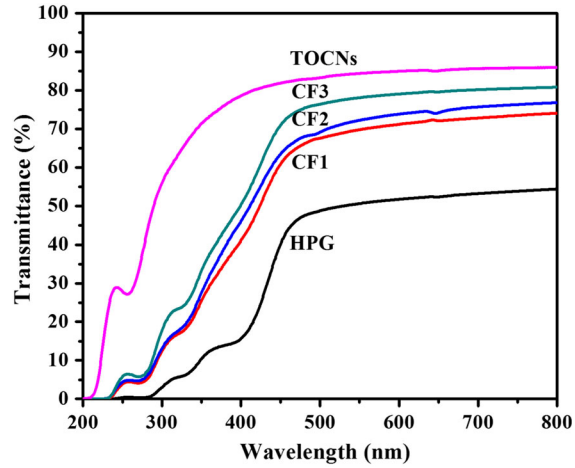

Fig. 2 UV-Vis transmittance of films made from HPG and TOCNs

The moisture content, thickness, density and tensile properties of the films with various HPG/TOCNs ratios are listed in Table 1. Moisture content of the films was determined by drying the samples in an oven at 105 °C for 5 h. The moisture content of the

Fig. 1 Photographs of control (nothing covered) and films made from HPG and TOCNs

Table 1 Physical and tensile properties of films prepared from TOCNs and HPG

	Moisture content (%)	Thickness (μm)	Density (g/cm^3)	Tensile strength (MPa)	Elongation (%)
HPG film	15.63	106.8 ± 1.4	1.06 ± 0.01	19.1 ± 1.0	7.23 ± 0.50
CF1	14.10	96.4 ± 1.4	1.17 ± 0.02	39.8 ± 4.5	6.64 ± 0.42
CF2	13.57	82.5 ± 0.5	1.37 ± 0.01	44.6 ± 4.3	5.62 ± 0.24
CF3	12.92	70.2 ± 2.9	1.45 ± 0.06	51.6 ± 1.6	4.13 ± 0.30
TOCNs film	12.72	61.1 ± 0.7	1.52 ± 0.02	149.9 ± 13.8	2.21 ± 0.47

composite films was decreased with the increase of TOCNs content, indicating that cellulose fibers might have lower affinity to water than HPG. The density of the film was increased and thickness was decreased with the increase of TOCNs content, suggesting that the TOCNs content affected the pore size and cracks in the composite film. Pure HPG film showed the lowest tensile strength of around 20.0 MPa and the tensile strength of the composite films was increased with the increase of TOCNs content. Meanwhile, the elongation at break of the films was decreased dramatically with the increase of TOCNs content. The highest tensile strength of 149.9 MPa was found in pure TOCNs film. The high tensile strength of the TOCNs film may be attributed to its high crystallinity, large aspect ratio of nanofibrils (Fukuzumi et al. 2009; Wu et al. 2012) and the numerous O···HO hydrogen bonds formed between its elements (Shimizu et al. 2014). The high crystallinity, large aspect ratio and uniform distribution of TOCNs can also significantly improve the mechanical properties of its composite film (Jradi et al. 2012; Wu et al. 2012; Zhou et al. 2012). The denser structure caused by the addition of TOCNs may also contribute to the increased tensile strength of the composite films (Kong et al. 2014; Takagi and Asano 2008; Qing et al. 2012). The enhanced tensile strength of the composite films might indicate the good interaction between HPG and TOCNs. Meanwhile, the incorporation of TOCNs could diminish the elongation at break of composite films. The stiffness of TOCNs as well as the low moisture contents in the composite films with higher TOCNs contents may lead to their low elongation (Fujisawa et al. 2011).

Miscibility

The IR spectrum of a blend of two compatible polymers should be significantly different from their individual IR spectra. And the differences, including band shifts, intensity changes and peak broadening, are derived from chemical interactions (Dong and Ozaki 1997; Xiao et al. 2003). Figure 3 shows the IR spectra of HPG, TOCNs and CF2 films. The broad absorption band of HPG at 3650–3000 cm^{-1} could be assigned to the stretching of O–H. The bands at 2920 cm^{-1} was ascribed to C–H stretching. The peak at 3340 cm^{-1} in the spectrum of pure TOCNs film was attributed to the characteristic peak of hydroxyl groups. However, the intensity of O–H stretching vibration band was lower due to the oxidation of the primary hydroxyl at C6 (Wang et al. 2014b). The peak at ~1600 cm^{-1} was attributed to the C=O stretching vibration of sodium carboxylate groups (Homma et al. 2013; Fukuzumi et al. 2013a). The corresponding absorption peaks of composite film CF2, including O–H stretching, C–H stretching and C=O stretching appeared at 3343, 2900 and 1602 cm^{-1}, respectively. Based on the increased intensity of O–H absorption peak and the peak shift of sodium carboxylate group, it could be concluded that HPG and TOCNs were cross-linked.

Figure 4 shows the SEM images of the cross-sections of all films. Numerous pores and cracks were observed in HPG film. TOCNs film showed a dense and uniform compact structure. No big aggregates were observed in composite films. Their homogeneous morphology suggested that high miscibility occurred during the compositing and HPG had good adhesion to TOCNs. The interaction between HPG and TOCNs also led to the gradually decreased film thickness as the content of TOCNs increased. A rigid hydrogen-bond network of cellulose nanofibrils governed by percolation might also form in the composite films (Zhou et al. 2012).

Contact angle

Figure 5 shows the contact angle (CA) change of a water droplet on the films with the increase of

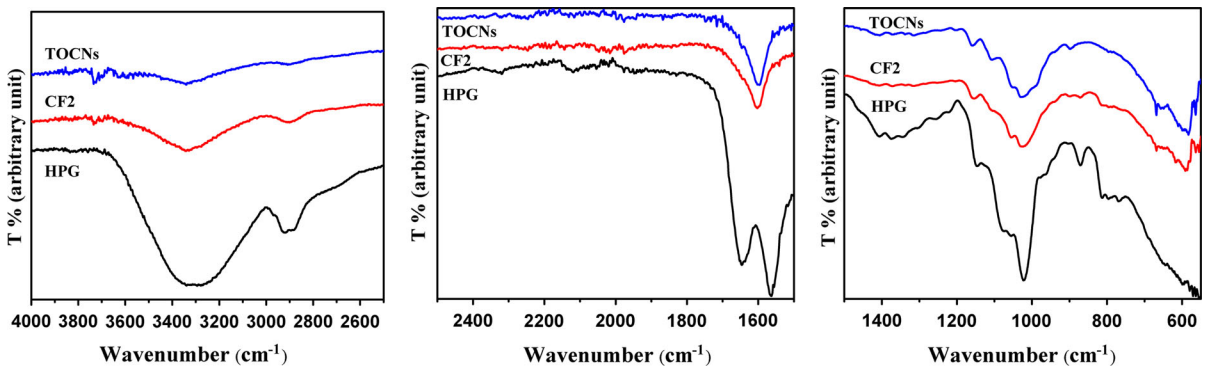

Fig. 3 FT-IR spectra of HPG, CF2, and TOCNs films

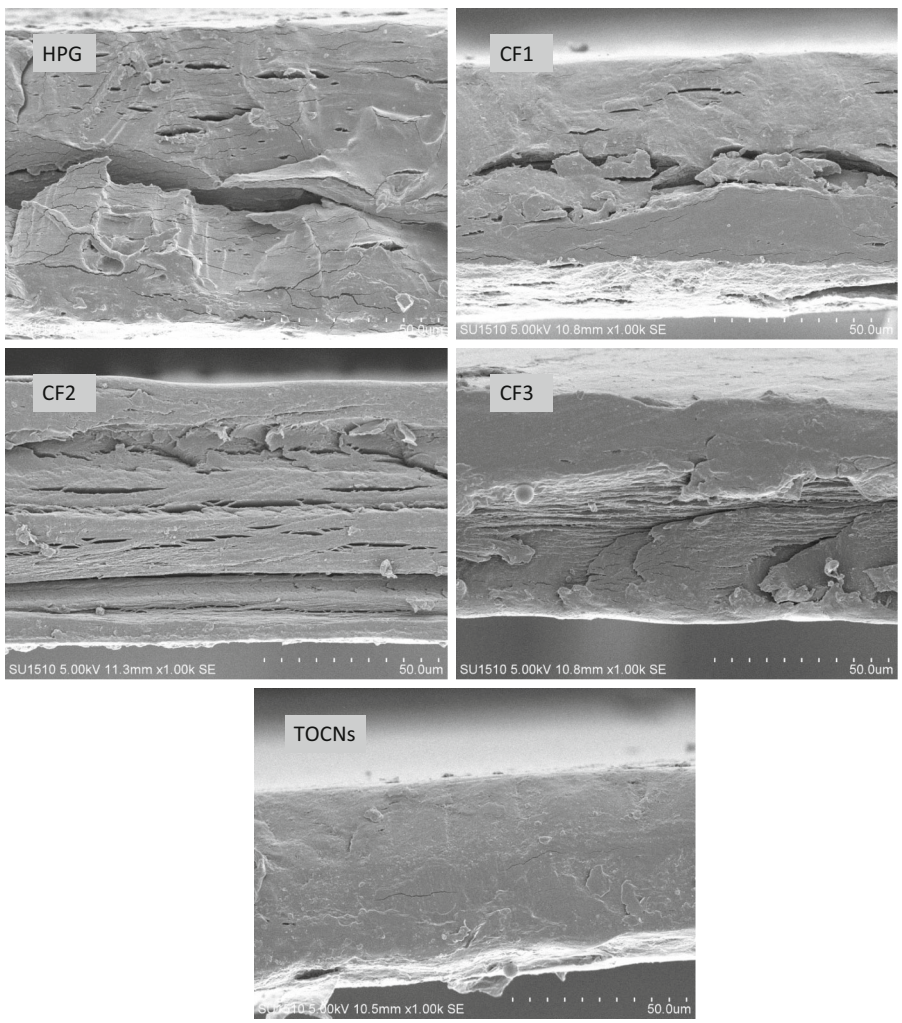

Fig. 4 SEM images of the cross-sections of pure HPG, pure TOCN, and composite films

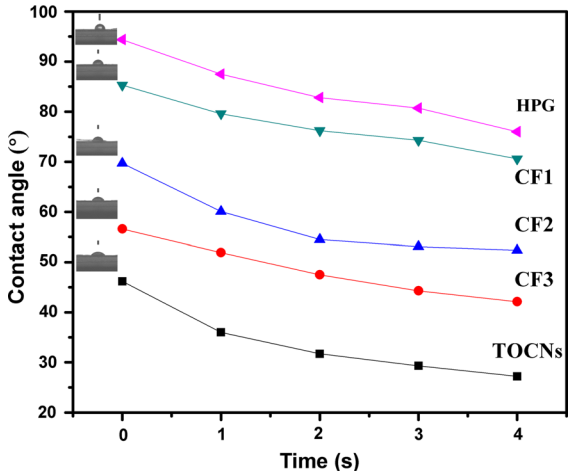

Fig. 5 Change in the contact angle with time of a water droplet on films

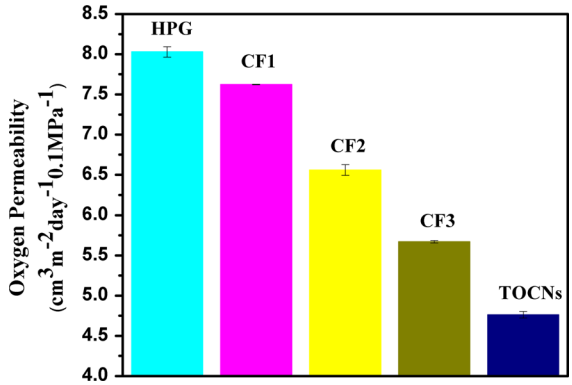

Fig. 6 Oxygen permeability of the films

contacting time. The surface roughness and chemical composition of a substrate can significantly affect its surface wettability (Rodionova et al. 2012a). The initial water contact angle of pure TOCNs film was 46.2°, consistent with the high hydrophilicity of the TOCNs film reported elsewhere (Fukuzumi et al. 2009). Otherwise, it was noticed that the pure HPG film had an initial water-contact angle of 94.4°. The water CAs of the composite films indicated that the incorporation of HPG significantly improved the surface water resistance of the composite films. Nevertheless, the different CAs of the composite films might also be partially attributed to their different surface roughness (Rodionova et al. 2012a; Wu et al. 2014). The CAs of the composite films decreased with the increase of contacting time due to the partial penetration of water into the films. For example, the CA of CF2 dropped to about 52.4° in 4 s. High water/moisture resistance is highly required for the application of TOCNs film as an oxygen-barrier packaging material (Kato et al. 2005). Therefore, the introduction of HPG can expand the application of TOCNs.

Oxygen-barrier and water vapor-barrier properties

All films including HPG, CF1, CF2, CF3 and TOCNs films were subjected to oxygen permeability measurements at 23 °C and 40 ± 1 % RH. The results are present in Fig. 6. The TOCNs film showed the lowest oxygen permeability of 4.76 cm^3 m^{-2} day^{-1}-0.1 MPa^{-1}. The regular chemical structures of the cellouronic acids in TOCNs film without bulky substituents or additives could contribute to its high oxygen-barrier level (Kato et al. 2005). Moreover, the high crystallinity and highly self-aligned elements in TOCNs film were also partially contribute to its superb oxygen-barrier property (Fukuzumi et al. 2013b; Rodionova et al. 2012c; Wu et al. 2012). The loose and cracked structure of pure HPG film diminished its oxygen barrier property. However, the oxygen permeability of TOCNs/HPG composite films was in the range of 5.67–7.62 cm^3 m^{-2} day^{-1}·0.1 MPa^{-1} (Fig. 6). The large amount of sodium carboxyl and hydroxyl groups in TOCNs could form denser aggregates alone or with HPG through strong intra- and inter-molecular hydrogen bond, which increased the oxygen barrier of the composite films (Kato et al. 2005). Moreover, water can act as a permeation medium for gases. Therefore, the reduced moisture content caused by the introduction of TOCNs to the composite films also improved their oxygen barrier (Sharma et al. 2014). In all, the HPG/TOCNs composite films still showed excellent oxygen-barrier properties and could be used as an oxygen sensitive food packaging.

The WVP of all films is given in Fig. 7. The WVP values of TOCNs and HPG films were 1.17×10^{-5} g m/(m^2 day Pa) and 0.53×10^{-5} g m/(m^2 day Pa), respectively. As discussed above, HPG has higher water affinity than cellulose fibers. However, it has been reported that guar gum can effectively trap and retain the water molecules within a matrix (Rosiaux et al. 2013; Poinot et al. 2014). Guar gum film shows

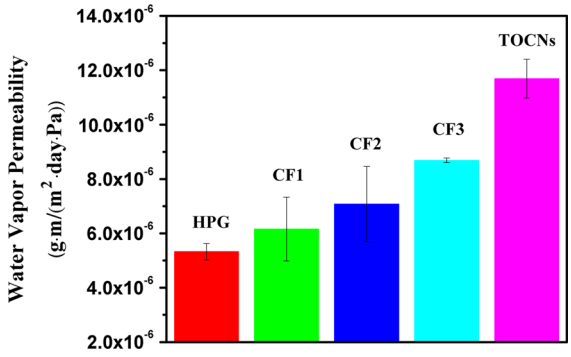

Fig. 7 Water vapor permeability of films

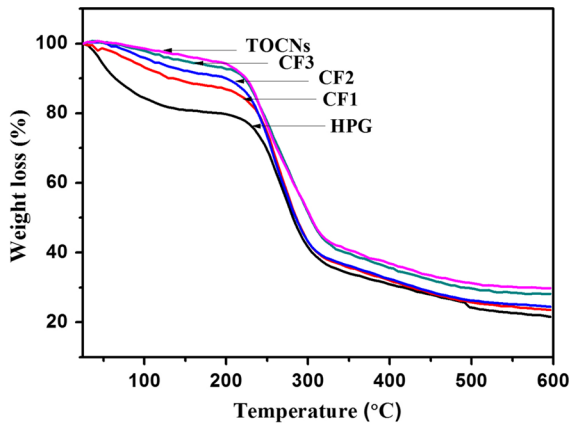

Fig. 8 TGA curves of neat HPG film, TOCNs film and composite films

pronounced desorption hysteresis in equilibrium moisture content and can act as barrier to air and moisture (Keating et al. 2013; Shetty et al. 1996). The composite films showed lower WVP than TOCNs film, indicating that the introduction of HPG effectively reduced the WVP of the composite films. Mueller et al. (2009) found that the water vapor barrier of starch/cellulose films was improved as the film density reduced from 2.41 $\times$ 10^6 to 1.31 $\times$ 10^6 g/m^3. Therefore, the lower density of the composite film might also partially contribute to its decreased WVP.

Thermal stability of the films

The thermal behaviors of HPG, TOCNs and HPG/TOCNs composite films were investigated by thermogravimetric analysis (TGA). All films subjected to a weight loss in the temperature range of 50–110 °C, which was attributed to their moisture contents (Fig. 8). The second weight loss of HPG film was observed at 240 °C where the polymer decomposition occurred (Nayak and Singh 2001). Further increasing the temperature to 330 °C led to increased weight loss rate. Thermal degradation of TOCNs film appeared at 200 °C where the crystalline phase of TOCNs was destroyed and the amorphous phase was decomposed into mono-D-glucopyranose (Rodionova et al. 2012b; Jradi et al. 2012). The third weight loss at 360–600 °C was attributed to the carbonation (Wang et al. 2014a). The decomposition temperature for the composite films, i.e., CF1, CF2 and CF3 were 223, 217 and 210 °C, respectively, indicating that the thermal stability of the composite films was increased with the increase of HPG content. The high thermal stability of composites could be attributed to the hydrogen bonds formed between the –OH and –COO$^-$ groups of TOCNs and the –OH groups of HPG (Xiao et al. 2003).

Conclusions

A new transparent high gas-barrier composite film was prepared from hydroxypropyl guar (HPG) and TEMPO-oxidized cellulose nanofibrils (TOCNs) by a solution casting method. The morphologies, tensile strength, water resistance, oxygen permeability, water vapor permeability and thermal stability were investigated. The results indicate that the composite films have excellent mechanical property, as well as high oxygen and water vapor barrier properties. The bending mass ratio of HPG to TOCNs can significantly affect their properties. The HPG/TOCNs composite films can be used as wholly biomass-sourced films for the food and medicine packaging.

Acknowledgments This study was supported by the National Natural Science Foundation of China (31270633), Creative Fund of Combination of Industry, Academia and Research of Jiangsu Province, China-Prospective Joint Research Project (BY2013015-03), the Natural Science Foundation of Hebei Province of China (B2013210032), and the Natural Science Foundation of Jiangsu Province of China (BK20140145).

References

Aulin C, Strom G (2013) Multilayered alkyd resin/nanocellulose coatings for use in renewable packaging solutions with

a high level of moisture resistance. Ind Eng Chem Res 52(7):2582–2589

Cheng Y, Brown KM, Prud'homme RK (2002) Characterization and intermolecular interactions of hydroxypropyl guar solutions. Biomacromolecules 3(3):456–461

Dai L, Long Z, Lv Y, Feng Q-C (2014) The role of formic acid pretreatment in improving the carboxyl content of TEMPO-oxidized cellulose. Cellul. Chem Technol 5–6(48):469–475

Das D, Ara T, Dutta S, Mukherjee A (2011) New water resistant biomaterial biocide film based on guar gum. Bioresour Technol 102(10):5878–5883

Dong J, Ozaki Y (1997) FTIR and FT-Raman studies of partially miscible poly(methyl methacrylate)/poly(4-vinylphenol) blends in solid states. Macromolecules 30(2):286–292

Fujisawa S, Okita Y, Fukuzumi H, Saito T, Isogai A (2011) Preparation and characterization of TEMPO-oxidized cellulose nanofibril films with free carboxyl groups. Carbohydr Polym 84(1):579–583

Fukuya MN, Senoo K, Kotera M, Yoshimoto M, Sakata O (2014) Enhanced oxygen barrier property of poly(ethylene oxide) films crystallite-oriented by adding cellulose single nanofibers. Polymer 55(22):5843–5846

Fukuzumi H, Saito T, Iwata T, Kumamoto Y, Isogai A (2009) Transparent and high gas barrier films of cellulose nanofibers prepared by TEMPO-mediated oxidation. Biomacromolecules 10(1):162–165

Fukuzumi H, Fujisawa S, Saito T, Isogai A (2013a) Selective permeation of hydrogen gas using cellulose nanofibril film. Biomacromolecules 14(5):1705–1709

Fukuzumi H, Saito T, Isogai A (2013b) Influence of TEMPO-oxidized cellulose nanofibril length on film properties. Carbohydr Polym 93(1):172–177

Homma I, Fukuzumi H, Saito T, Isogai A (2013) Effects of carboxyl-group counter-ions on biodegradation behaviors of TEMPO-oxidized cellulose fibers and nanofibril films. Cellulose 20(5):2505–2515

Iwatake A, Nogi M, Yano H (2008) Cellulose nanofiber-reinforced polylactic acid. Compos Sci Technol 68(9): 2103–2106

Jradi K, Bideau B, Chabot B, Daneault C (2012) Characterization of conductive composite films based on TEMPO-oxidized cellulose nanofibers and polypyrrole. J Mater Sci 47(8):3752–3762

Kato Y, Kaminaga J, Matsuo R, Isogai A (2005) Oxygen permeability and biodegradability of polyuronic acids prepared from polysaccharides by TEMPO-mediated oxidation. J Polym Environ 13(3):261–266

Keating BA, Hill CAS, Sun DY, English R, Davies P, McCue C (2013) The water vapor sorption behavior of a galactomannan cellulose nanocomposite film analyzed using parallel exponential kinetics and the Kelvin-Voigt viscoelastic model. J Appl Polym Sci 129(4):2352–2359

Kong LL, Zhang DL, Shao ZQ, Han BX, Lv YX, Gao KZ, Peng XQ (2014) Superior effect of TEMPO-oxidized cellulose nanofibrils (TOCNs) on the performance of cellulose triacetate (CTA) ultrafiltration membrane. Desalination 332(1):117–125

Kurihara T, Isogai A (2014) Properties of poly(acrylamide)/TEMPO-oxidized cellulose nanofibril composite films. Cellulose 21(1):291–299

Lu C, Kostanski L, Ketelson H, Meadows D, Pelton R (2005) Hydroxypropyl guar-borate interactions with tear film mucin and lysozyme. Langmuir 21(22):10032–10037

Mueller CMO, Laurindo JB, Yamashita F (2009) Effect of cellulose fibers addition on the mechanical properties and water vapor barrier of starch-based films. Food Hydrocoll 23(5):1328–1333

Nayak BR, Singh RP (2001) Synthesis and characterization of grafted hydroxypropyl guar gum by ceric ion induced initiation. Eur Polym J 37(8):1655–1666

Poinot T, Govin A, Grosseau P (2014) Importance of coil-overlapping for the effectiveness of hydroxypropylguars as water retention agent in cement-based mortars. Cement Concr Res 56:61–68

Qi ZD, Saito T, Fan YM, Isogai A (2012) Multifunctional coating films by layer-by-layer deposition of cellulose and chitin nanofibrils. Biomacromolecules 13(2):553–558

Qing Y, Sabo R, Wu YQ, Cai ZY (2012) High-performance cellulose nanofibril composite films. BioResources 7(3):3064–3075

Rodionova G, Eriksen Ø, Gregersen Ø (2012a) TEMPO-oxidized cellulose nanofiber films: effect of surface morphology on water resistance. Cellulose 19(4):1115–1123

Rodionova G, Roudot S, Eriksen Ø, Männle F, Gregersen Ø (2012b) The formation and characterization of sustainable layered films incorporating microfibrillated cellulose (MFC). Bioresources 7(3):3690–3700

Rodionova G, Saito T, Lenes M, Eriksen Ø, Gregersen Ø, Fukuzumi H, Isogai A (2012c) Mechanical and oxygen barrier properties of films prepared from fibrillated dispersions of TEMPO-oxidized norway spruce and eucalyptus pulps. Cellulose 19(3):705–711

Rosiaux Y, Muschert S, Chokshi R, Leclercq B, Siepmann F, Siepmann J (2013) Ethanol-resistant polymeric film coatings for controlled drug delivery. J Control Release 169(1–2):1–9

Saito T, Nishiyama Y, Putaux J-L, Vignon M, Isogai A (2006) Homogeneous suspensions of individualized microfibrils from TEMPO-catalyzed oxidation of native cellulose. Biomacromolecules 7(6):1687–1691

Saito T, Kimura S, Nishiyama Y, Isogai A (2007) Cellulose nanofibers prepared by TEMPO-mediated oxidation of native cellulose. Biomacromolecules 8(8):2485–2491

Sharma S, Zhang XD, Nair SS, Ragauskas A, Zhu JY, Deng YL (2014) Thermally enhanced high performance cellulose nano fibril barrier membranes. RSC Adv 4(85):45136–45142

Shetty CS, Bhaskar N, Bhandary MH, Raghunath BS (1996) Effect of film-forming gums in the preservation of salted and dried Indian mackerel (Rastrelliger kanagurta cuvier). J Sci Food Agric 70(4):453–460

Shimizu M, Saito T, Fukuzumi H, Isogai A (2014) Hydrophobic, ductile, and transparent nanocellulose films with quaternary alkylammonium carboxylates on nanofibril surfaces. Biomacromolecules 15(11):4320–4325

Sirvio JA, Kolehmainen A, Visanko M, Liimatainen H, Niinimaki J, Hormi OEO (2014) Strong, self-standing oxygen barrier films from nanocelluloses modified with regioselective oxidative treatments. ACS Appl Mater Interfaces 6(16):14384–14390

Song ZP, Xiao HN, Zhao Y (2014) Hydrophobic-modified nano-cellulose fiber/PLA biodegradable composites for

lowering water vapor transmission rate (WVTR) of paper. Carbohydr Polym 111:442–448

Takagi H, Asano A (2008) Effects of processing conditions on flexural properties of cellulose nanofiber reinforced "green" composites. Compos Part A-Appl S 39(4):685–689

Wang F, Kim S-S, Kee C-D, Shen Y-D, Oh I-K (2014a) Novel electroactive PVA-TOCN actuator that is extremely sensitive to low electrical inputs. Smart Mater Struct 23(7): 1–10

Wang Z, Ma HY, Hsiao BS, Chu B (2014b) Nanofibrous ultrafiltration membranes containing cross-linked poly(-ethylene glycol) and cellulose nanofiber composite barrier layer. Polymer 55(1):366–372

Wu XY, Ye YQ, Chen YN, Ding B, Cui JJ, Jiang B (2010) Selective oxidation and determination of the substitution pattern of hydroxypropyl guar gum. Carbohydr Polym 80(4):1178–1182

Wu C-N, Saito T, Fujisawa S, Fukuzumi H, Isogai A (2012) Ultrastrong and high gas-barrier nanocellulose/clay-layered composites. Biomacromolecules 13(6):1927–1932

Wu C-N, Saito T, Yang QL, Fukuzumi H, Isogai A (2014) Increase in the water contact angle of composite film surfaces caused by the assembly of hydrophilic nanocellulose fibrils and nanoclay platelets. ACS Appl Mater Interfaces 6(15):12707–12712

Xiao CB, Zhang JH, Zhang ZJ, Zhang LN (2003) Study of blend films from chitosan and hydroxypropyl guar gum. J Appl Polym Sci 90(7):1991–1995

Yang H, Tejado A, Alam N, Antal M, van de Ven TG (2012) Films prepared from electrosterically stabilized nanocrystalline cellulose. Langmuir 28(20):7834–7842

Yano H, Sugiyama J, Nakagaito AN, Nogi M, Matsuura T, Hikita M, Handa K (2005) Optically transparent composites reinforced with networks of bacterial nanofibers. Adv Mater 17(2):153–155

Zhou YM, Fu SY, Zheng LM, Zhan HY (2012) Effect of nanocellulose isolation techniques on the formation of reinforced poly(vinyl alcohol) nanocomposite films. Express Polym Lett 6(10):794–804